Applications of Infrared Free-Electron Lasers: Basic Research on the Dynamics of Molecular Systems

Dana D. Dlott and Michael D. Fayer

Invited Paper

Abstract—**Applications of tunable infrared (IR) picosecond (ps) pulses generated by free-electron lasers (FEL's) are considered from several perspectives. First, general considerations are presented that discuss characteristics that an IR ps FEL must have to be successfully used as an optical source in order to perform complex ultrafast experiments commonly undertaken with conventional ps lasers. The features that FEL's can have that will make them superior to conventional sources for the investigation of complex molecular systems in condensed and gas phases are pointed out, and the difficulties of combining an FEL with an intricate experimental apparatus are brought forward. Next, ps photon echo experiments on a near-IR dye molecule in a low-temperature glass, performed using the Stanford superconducting linear accelerator-pumped FEL, are discussed to illustrate the ability of FEL's to act as light sources for sophisticated applications. The methods employed and the problems encountered in the echo experiments are described. Finally, the applications of IR ps FEL's to the study of molecular vibrational dynamics are discussed, including detailed numerical feasibility calculations. It is shown how to determine the extent of vibrational excitation for a given system, given readily determined molecular and FEL parameters; substantial excited vibrational populations can be generated in the examples considered. Once a vibration is excited, a variety of methods of probing the subsequent dynamics are discussed. These include absorption probing (pump-probe experiment), probing by anti-Stokes Raman scattering, and probing by hyper-Raman scattering. A class of experiments referred to as nanoheating, i.e., selective heating on a nanometer length scale, is described. Biomedical and biophysical applications of nanoheating are suggested.**

I. Introduction

FREE-ELECTRON lasers (FEL's) have developed rapidly in the last 15 years [1], and many applications for them have been envisioned [2]–[4]. To use the output of an FEL for fundamental studies of condensed-phases and gas-phase molecular systems requires both an optical source that meets stringent requirements and the mating of that source with an experimental apparatus. A laser by itself is not capable of making meaningful measurements. An FEL application may involve an experimental apparatus with complexity approaching that of the FEL.

In recent years, laser spectroscopy using conventional lasers has become very sophisticated [5], [6], and with this sophistication, the demands routinely placed on these lasers have grown. FEL operation at a wide variety of wavelengths has been demonstrated [1], [4], but the capability of simultaneously and reliably fulfilling the necessary demanding operational specifications to conduct sophisticated experiments is not straightforward. It is a challenge to the FEL community to harness the unique capabilities of FEL's to realize the vast potential of suggested applications and to make FEL's into potent tools for basic research. In order to attain this goal, FEL developers and users must develop a relationship that can ultimately lead to the realization of these applications and to the development of better FEL's.

In this paper, we focus on applications of tunable infrared (IR) picosecond (ps) pulses in the study of dynamics of molecular systems. Infrared FEL's are at this time the most highly developed and reliable systems that offer clear advantages over available benchtop lasers. The examples presented here include the dynamics of condensed matter (e.g., solids and surfaces), gas-phase dynamics, and medical and biological applications. All these systems involve the interactions of many bodies, and therefore they present a rich variety of dynamical phenomena occurring on the ultrafast time scale.

There are two additional reasons for our focus on infrared applications. IR spectroscopy [7], [8] is intrinsically interesting and valuable, and it seems hardly worthwhile to consider FEL applications in the visible and near UV, where an enormous variety of high-power benchtop laser systems are available from commercial sources. The most important spectral region for chemical applications is the vibrational IR (3–30 μm), although many interesting applications involve the near IR (1–3 μm). The dynamics of transitions in the far IR (30–200 μm) are of undisputable importance but are barely explored.

Intense IR pulses can be applied in three canonical applications. The first is the study of electronic transitions of materials with small energy gaps. These include a variety of semiconductors, particularly those like HgCdTe, which are used in IR detectors, high T_c superconductors, and large organic and inorganic molecules with low-lying electronic states. The second is the study of mechanical excitations. These include phonons and vibrons, which

Manuscript received March 27, 1991; revised July 13, 1991. This work was supported by the National Science Foundation, Division of Materials Research by Grant DMR 87-21253, the U.S. Army Research Office by Grant DAALO-90-G-0030 (to D.D.D.), by the MFEL program through the Office of Naval Research by Grant N00014-89-K0154, and by National Science Foundation, Division of Materials Research by Grant DMR 87-18959 (to M.D.F).

D. D. Dlott is with the School of Chemical Sciences, University of Illinois, Urbana, IL 61801.

M. D. Fayer is with the Department of Chemistry, Stanford University, Stanford, CA 94305.

IEEE Log Number 9103642.

are collective modes of crystalline solids, and vibrations localized on individual molecules. Molecular vibrations are sensitive to the details of the structure of a molecule, and therefore provide fingerprint selectivity in molecular identification [7], [8]. Selective excitation of a specific molecular vibration may provide a route to the control [9] of the chemical reactivity of that molecule. Molecular vibrational spectroscopy can be used to investigate crystalline and amorphous solids, liquids, molecules on surfaces, and systems of biological or biomedical interest. The third type of application involves nanoheating, i.e., transient heating of nanoscale structures. The FEL differs from ordinary heat sources in its ability to excite one component of a complex mixture via vibrational selectivity to thereby produce a substantial jump in temperature of exceedingly brief duration.

Ultrashort light pulses are of fundamental importance in probing the dynamics of complicated systems [5], [6]. An elementary argument in statistical mechanics can be used to show that the limiting time scale of most mechanical processes is of order $h/k_BT \approx 10^{-13}$ s at ambient temperature. Practically every mechanical and chemical process of interest, including relaxation processes, energy transfer, and chemical reactions, occurs slower than 100 fs. The pulse duration produced by most FEL's is only one order of magnitude greater than this characteristic time, thus opening up a window to a substantial variety of dynamical processes. A number of proposals have been advanced to achieve the remaining order of magnitude, including optical pulse compression [10] using IR-transmitting optical fibers.

Because reliability of existing FEL's is always a pressing issue, we believe there is a tendency in the FEL community to imagine that compared to operating the FEL, FEL applications are straightforward. We wish to stress the rigorous and demanding nature of the application, i.e., the experimental setup, which exploits the unique properties of FEL's. A successful application will not only advance our understanding of the material at hand but also provide insight into the detailed behavior of the FEL by demanding a high level of performance from the FEL.

In the following, we will discuss the performance specifications we believe are required for a successful applications program. At one time or another, most existing FEL's have already met one or more of these specifications. The real challenge is meeting the combination of them required for a given experiment. We then present a real-world example where the superconducting accelerator-pumped FEL at Stanford University (hereafter denoted SCA/FEL) was used to perform a complex series of experiments to measure nonlinear and coherent optical transients in an amorphous solid. This example is quite encouraging for the prospects of future applications, but it also demonstrates the difficulties FEL designers face in obtaining the required level of performance. Then we discuss quantitative experimental considerations that go into deciding whether a particular application is feasible. Finally, we present some selected examples of proposed applications. These applications were chosen using three criteria. They are expected to provide scientifically interesting and unique information about important materials, they cannot reasonably be performed using available benchtop laser systems, and there is a high probability of success using existing FEL sources.

II. Free-Electron Laser Applications: Specifications for Applications

In this section we investigate the performance specifications an FEL must achieve to be useful in sophisticated applications. In many cases it has been demonstrated that a particular FEL can deliver a substantial (time averaged) power at a convenient center wavelength. This type of measurement does not characterize FEL performance in enough detail to determine whether an FEL is capable of performing a specific application.

The most important attribute of an FEL is reliable performance. At this time the greatest obstacle to all FEL applications is the lack of availability of FEL photons. It is also important to keep in mind that an FEL is simply a laser. There is a fundamental difference between an FEL facility and a synchrotron light source in the FEL's inability to service many users. The power supplied by a synchrotron light source is independent of the number of user ports. Furthermore, a synchrotron radiation light source provides polychromatic radiation so each user has the ability to select from a wide range of wavelengths.

Experience acquired using conventional lasers indicates that sharing a laser among many users can be quite difficult. Benchtop lasers generally service a single experiment at one time. Sharing is further inhibited by tunable lasers as different users will typically need pulses at different wavelengths. Although in some situations it may be possible, it is generally unlikely that two or more experiments using an FEL can be performed simultaneously.

However, an FEL facility can service more users than a benchtop laser. Because an FEL typically costs 10–100 times as much as even a sophisticated benchtop laser or an experimental setup, economies of scale indicate that the cost of an FEL is not greatly increased by having the FEL service several independent experimental setups *sequentially*, located in individual user areas. Because an IR FEL is easily tuned by varying the electron beam energy, FEL's may be rapidly scanned over a broad wavelength range limited only by the optical components in use. In the sequential user paradigm, each user commands the FEL at the wavelength of choice for a given time period, and then command is shifted to another user. The premium placed on FEL photons demands that each user's apparatus be prealigned to the greatest extent possible, probably by use of an alignment laser made collinear with the FEL beam.

Some ingenious schemes have been proposed to provide for simultaneous *parallel* use of a FEL. For example, the electron beam energy can be modulated so that

successive micropulses [11] or macropulses have different wavelengths. Then a beam-switching system can be used to direct different frequency pulses into different experiments. The drawback of these schemes is reduced repetition rate and reduced power at a particular experimental station.

Economic realities suggest that FEL applications be generally limited to cases where the FEL provides a *significant* performance advantage over conventional laser systems. FEL users have a right to expect that the cost in time and money of travel to an FEL facility should be rewarded by data that cannot be obtained at the home base. For this reason, it seems senseless to contemplate FEL applications in the visible and near UV where a wide variety of commercial ps laser systems are available. For example, a recently developed amplified dye laser system using a high repetition rate solid-state regenerative amplifier [12] is capable of producing, in the visible and in the near-UV by frequency doubling, tunable sub ps pulses of cal 1 mJ output energy at 1000 pps (i.e., 1 W) for roughly $350 000.

Picosecond pulse tunable lasers in the vibrational IR are not yet available commercially but may be assembled from mostly commercial components. Conventional laser systems produce tunable IR pulses using one of two methods. 1) Solid-state laser pump with parametric generation and optical parametric amplification (OPO), or 2) difference frequency mixing of a solid-state laser with a tunable dye laser in a nonlinear crystal [6], [13]. At this time, most systems use either $LiNbO_3$ or $LiIO_3$, which limits the red edge of the tuning range to roughly 5 μm. The time-averaged power of the largest of these systems does not exceed a few milliwatts, and the cascade of nonlinear processes required to produce tunable IR leads to amplitude noise that is considerably greater than that expected from a good solid-state laser system or a properly functioning FEL.

In Table I we have listed some performance specifications that an FEL-based user facility should meet in order to be useful for demanding applications. Our philosophy is that the performance of FEL in the IR should be comparable to that expected from a good benchtop laser system in the visible and should substantially outperform any existing ultrashort pulse IR laser system.

Three particular attributes in Table I are worthy of comment—the micropulse spacing, the IR frequency specifications, and the amplitude stability. A micropulse spacing smaller than a few nanoseconds is highly undesirable. The frequency characteristics of the FEL pulse are a much overlooked but critical parameter for many applications. Also FEL's appear to offer a significant advantage in amplitude stability relative to most benchtop lasers.

In practically all applications, the system of interest must be allowed to relax back to equilibrium after each pump pulse. When the micropulse spacing becomes comparable to the characteristic relaxation time, bottleneck and accumulation effects are produced that greatly complicate the interpretation of experimental results (although in certain cases, these effects may be of interest themselves). The historical example of lifetime measurements of the dye, denoted DODCI, present an excellent example. Literature values of this lifetime in the early 1970's varied by more than one order of magnitude [14]. The variation was later attributed to multiple pulse effects when many pulses of a mode-locked pulse train were used, rather than a single pulse selected by a fast optical switch.

It is critically important to be able to determine that a particular effect is independent of micropulse spacing. Micropulse spacing can be controlled by an external single-pulse selector. When the micropulse spacing is less than a few nanoseconds, it becomes difficult to select a single pulse, even using the fastest available electrooptic modulator (EOM) technology. The 85 ns spacing of the SCA/FEL is particularly attractive since an inexpensive, convenient acoustooptic modulator (AOM) can be used.

TABLE I
PERFORMANCE PARAMETERS REQUIRED FOR FEL APPLICATIONS

Reliability	High	Simpler applications can wait for the FEL. More sophisticated applications require more reliability
Pointing stability	Beam movement should be limited to a few percent of the diameter at the applications platform	The FEL might be 100 m from the applications platform. Active control with feedback may be required
Beam quality	Single mode, preferably TEM_{00}	Beam quality of FELs is typically excellent, but not necessarily TEM_{00}
Micropulse energy	>1 μJ	See feasibility calculations in Section IV.
Micropulse duration	<10 ps	<10 ps is adequate for many applications. But pulse width jitter must be avoided.
Micropulse spacing	>10 ns	Spacing between adjacent micropulses must exceed the rise time of available electrooptic modulators
Time-averaged power	>1 W	Must exceed existing benchtop systems by at least $10\times$
Amplitude stability	$\pm 10\%$	A typical specification for a tunable ultrafast laser
Frequency bandwidth $\Delta\nu$	Close to the transform limit	0.15% of λ_0 at 3.3 μm for a 3-ps pulse
Frequency jitter	Small compared to $\Delta\nu$	Frequency chirp during the macropulse is a severe hindrance to any application involving sharp molecular or atomic transitions
Frequency accuracy	Large compared to $\Delta\nu$	Operator must be able to lock FEL onto a transition with linewidth $<\Delta\nu$ for extended time periods

But any micropulse separation greater than 10 ns makes single-pulse selection relatively straightforward.

In many applications, a user will wish to lock the FEL onto a particular narrow atomic or molecular transition. Frequently, the width of a transition $\Delta\nu$ will be smaller than the transform-limited width of the micropulse $\Delta\nu_L$. So a high degree of precision (typically better than 0.1%) is required in setting and maintaining the center frequency ν_L of the FEL. A problem may develop in communicating the users' needs to the FEL operator, who tunes the FEL by varying the energy of the electron beam. A Fourier-transform IR spectrometer with a stabilized He–Ne laser reference could be quite useful because it provides reproducible, absolute frequency precision. Alternatively, an IR detector may be used to monitor the transmission of the FEL beam through the users' sample, and this information is fed back to the FEL operator.

A notable observation from the experimental work reported in Section III [15], [16] is that the amplitude stability of an IR FEL can be surprisingly good, particularly when compared to benchtop sources of tunable IR pulses. In benchtop sources, dye lasers and nonlinear frequency shifting crystals are additional sources of noise apart from the master laser oscillator. But a less recognized advantage of FEL's appears to be the ease of additional external amplitude stabilization. In [16], a feedback circuit using acoustooptic modulators with a 10 μs response was able to stabilize an FEL within 1%. The ease of stabilization was attributed to the relatively low-frequency (< 10 kHz) amplitude fluctuations, compared to dye lasers that often have noise with a > 1 MHz bandwidth.

A point worth stressing is that all the performance specifications in Table I must be met *simultaneously* for many applications. Different FEL designs produce different instabilities, and a solution that reduces a particular instability must not be allowed to significantly degrade another desirable property. For example, some FEL designs produce a chirped macropulse. Therefore, only a small fraction of the micropulses produced in a given macropulse may excite a transition of interest, resulting in a substantial loss of *effective* average power.

In light of the above discussion, an IR FEL is the instrument of choice when it offers a significant advantage over the more readily available benchtop laser systems. The advantages may be technical in nature, but they may also be logistical. The benchtop systems discussed here are neither inexpensive nor simple to operate. Thus an FEL center can provide access to many users who otherwise would be unable to conduct their experiments. This is particularly true of users whose main experimental emphasis is not laser development. Referring to experiments performed with the SCA/FEL, the purely technical advantages may include:

1) Intense pulses to the red of 5 μm.

2) Pulses in the 1–5 μm region for applications where average power at the 1 W level is required.

3) Rapid scanning over a relatively large wavelength range.

4) Pulse-to-pulse stability typically better than OPO or dye lasers.

5) High repetition rate for efficient signal processing.

III. An Example: Nonlinear and Coherent Spectroscopy with a FEL

In this section we describe a sophisticated application of FEL radiation, namely picosecond photon echo experiments [15], [16] performed using the SCA/FEL at Stanford University [17]. Inasmuch as this application is of the same order of sophistication as any performed using benchtop laser systems, it provides valuable insight into the relationship between FEL developers and users and the level of performance required from the FEL. The ultimate success of this project can be attributed to a close interaction between users and FEL developers [17]. An expected consequence of this project was the use of the FEL to learn about condensed matter dynamics. An unexpected, but fortuitous, consequence was that feedback provided by the user gave the FEL operator new insight into the operation of the FEL [17].

In this series of preliminary experiments, the experimental conditions were carefully chosen to maximize the possibilities for success. The material under study, a near-IR absorbing dye HITCI (HITCI denotes 1,1′,3,3,3′,3′-hexamethylindotricarbocyanine iodide), had an extremely large absorption cross section ($\sigma_{pk} \approx 10^{-16}$ cm^2), to simplify the observation of coherent optical transients. The absorption spectrum of this dye molecule had a relatively large inhomogeneous linewidth of more than 100 cm^{-1}, requiring only that the FEL provide pulses at a single frequency within this band, not at any particular location [15]. In future applications, materials of interest may produce weaker signals, and the experiment may require the generation of a specific wavelength determined by the sample itself. Meeting these additional constraints appears reasonable with the apparatus at hand, but only experience can prove conclusively whether it is possible without introducing additional complications.

A. Frequency Doubling and Autocorrelation

In operating an FEL, it is important to have several diagnostic tools to verify the performance of the FEL. Most FEL facilities will have the basic instruments such as a fast photodetector, an oscilloscope, a slow-response power meter, and a spectrometer or spectrograph. But experience with ultrashort pulse laser systems shows that the performance of a laser cannot be adequately characterized without at least one more tool—an optical autocorrelator based on second harmonic generation (SHG) [6].

A block diagram of a conventional background free autocorrelator is shown in Fig. 1. The input pulse is split into two roughly equal amplitude pulses that overlap spatially at a SHG crystal with a variable temporal delay in one of the paths. The SHG crystal and detector are arranged so that only the SHG *sum* signal, i.e., the signal generated by one photon from each pulse, is detected. Be-

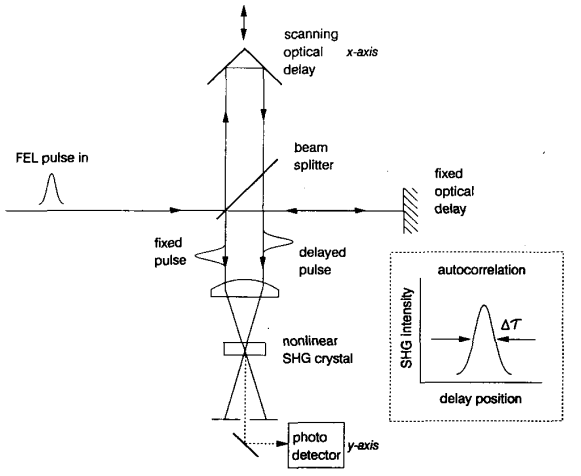

Fig. 1. Schematic diagram of a background-free ultrashort pulse autocorrelation apparatus. SHG denotes second harmonic generation. The delay is scanned through the region where the pulses overlap in time in the SHG crystal. Only the SHG signal generated by the pair of simultaneous pulses (dashed line) is detected. The individual pulses are not propagating in the phase-matched direction and do not themselves double.

cause the electronic response of the SHG crystal is essentially instantaneous, this sum signal only appears when the delay line permits the pulses to overlap temporally in the crystal. Ten millimeters of delay, or 60 ps, is typically sufficient. With some minor changes, the same optical arrangement is used in saturation recovery and photon echo experiments discussed below. In these cases the SHG crystal is replaced by the sample and the detector is moved to observe the intensity of the weaker of the two beams (saturation recovery) or the coherent emission emerging in a unique direction (photon echo).

In an autocorrelation measurement, scanning the optical delay τ produces an autocorrelation function $G^2(\tau)$ of width (FWHM) $\Delta\tau$. For the ideal case of a transform-limited Gaussian pulse [6],

$$t_p = 0.707\Delta\tau \tag{1a}$$

and

$$t_p \cdot \Delta\nu_l = 0.441 \tag{1b}$$

where t_p is the width of the input optical pulse. A deviation from the transform limit produces frequency substructure in the pulse, which can be resolved by careful autocorrelation measurement. The substructure appears as a short duration spike in the autocorrelation centered at $\tau = 0$ [6].

A variety of efficient SHG crystals are useful in IR applications [13]. SHG crystals serve not only as diagnostic tools but also as a means of extending the tuning range of an FEL to the short wavelength side. It is also clear that many applications require two-color operation, which in the absence of two lasers can be provided using the FEL fundamental and its second or higher harmonic. Materials of particular interest, and their effective range of transparency, include $LiNbO_3$ (1–4 μm), $LiIO_3$ (0.3–5.5 μm), CdS (0.5–15 μm), CdTe (1–28 μm), $AgGaS_2$ (1–11 μm), and $AgGaSe_2$ (1–22 μm).

In SHG, the power in the second harmonic, $P_{2\omega}$ is related to the input power in the fundamental P_ω by [18]

$$P_{2\omega} \propto (P_\omega)^2 \sin^2(\Delta kl/2)/(\Delta kl)^2 \tag{2}$$

where $(\Delta k)^{-1}$ is the characteristic length for phase matching of the fundamental and second harmonic wave, which depends on the material and the wave vectors and polarizations of the propagating waves, and l is the length of the SHG crystal. Equation (2) shows the efficient SHG occurs only under phase-matched conditions where $\Delta k \approx 0$.

The usual tool to study instabilities in an FEL is a fast photodetector and oscilloscope. Because these systems rarely have a bandwidth greater than one GHz, they can detect individual micropulses within a macropulse but cannot detect fluctuations in the duration of a micropulse. Even if micropulses appear stable on an oscilloscope, the intensity of the SHG pulses may be unstable due to instabilities in ν_L, $\Delta\nu_L$, and t_p. At constant micropulse energy, $P_{2\omega} \propto (t_p)^{-2} \cdot P_{2\omega}$ will also fluctuate if any fluctuating frequency components of the pulse lie outside the acceptance bandwidth of the SHG crystal. A typical acceptance bandwidth is a few cm^{-1} per cm of crystal length.

B. Results of FEL Autocorrelation Experiments

Autocorrelation and SHG measurements performed with the Stanford SCA/FEL [16], [17] revealed the importance of this diagnostic technique as well as some unique behavior of the FEL itself. Prior to these measurements, the optical cavity length had been adjusted to produce maximum optical power. Under these conditions, the intensity of the micropulse train at a 1.5 μm center wavelength was quite stable, to about 10% [17]. In an SHG measurement with a $LiIO_3$ crystal, the 0.75 μm second harmonic intensity fluctuated wildly compared to the 1.5 μm fundamental. The cause of the SHG instability was found to be multiple frequency components within each micropulse that were not stable in either amplitude or frequency [17]. The acceptance bandwidth of the SHG crystal being used translated the frequency fluctuations into readily observed SHG intensity fluctuations.

A subsequent readjustment of the FEL cavity length while observing the SHG power showed that by changing the cavity length by a few microns out of 12.7 m, the SHG output could be stabilized at the cost of reducing the average power by roughly a factor of two. In the stable configuration, the data shown in Fig. 2, reproduced from [16], were obtained.

In Fig. 2(b), the measured autocorrelation $G_2(\tau)$ is an excellent fit to a Gaussian function of width $\Delta\tau = 4.8$ ps, and therefore the pulsewidth is $t_p = 3.4$ ps. The measured spectrum of a single micropulse in Fig. 2(a) is also approximately Gaussian, of width $\Delta\nu_L = 4.5\ cm^{-1}$. The very

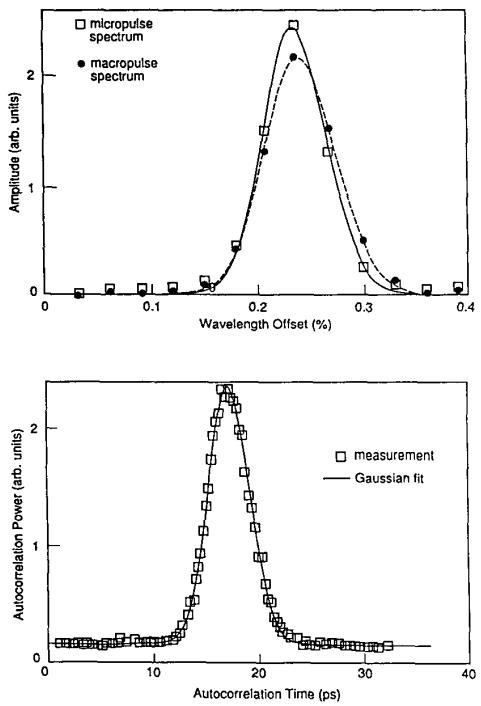

Fig. 2. Spectral and autocorrelation measurements performed on the SCA/FEL at Stanford University, reproduced from [16]. Top: The spectrum, centered at $\nu_L = 1.5$ μm of an entire macropulse, is only 10% wider than the width $\Delta\nu_L = 4.5$ cm^{-1} of a single micropulse. Bottom: the autocorrelation indicates a Gaussian pulse of duration $t_p = 3.4$ ps. The product $\Delta\nu_L t_p = 0.46$ is within 5% of the theoretical value of 0.441 for a transform-limited Gaussian pulse.

slight broadening of the macropulse spectrum of width $\Delta\nu_L = 5.0$ cm^{-1} indicates the virtual absence of frequency jitter during the macropulse. The product $\Delta\nu_L t_p = 0.46$, compared to the theoretical value from (1b) of 0.44, proves that these micropulses closely approximate the ideal Gaussian transform limited pulse.

This experiment provided a demonstration of the importance of diagnostic tools and interactions between FEL users and FEL developers. At the outset of the experiment, the FEL macropulse power (i.e., macropulse energy divided by macropulse duration) was believed to be 60 W. But the usable power, that is the power with stable SHG signal, proved to be 30 W [17]. This demonstrates the point made earlier: the performance parameters given in Table I that are necessary for a particular experiment must all be met *simultaneously*.

C. Picosecond Photon Echo Experiments Using the SCA/FEL

Photon echo spectroscopy [19]–[23] is a powerful method for studying condensed matter dynamics and intermolecular interactions. In the optical absorption spectrum of molecules in condensed matter systems, particularly at low temperature, there is often a contribution from static (or quasi-static) inhomogeneous broadening. This broadening contains no dynamical information. The photon echo pulse sequence removes inhomogeneous broadening, revealing the underlying dynamical or homogeneous broadening.

The FEL extends the wavelength range available for photon echo experiments. In the last few years, the Fayer group has studied the dynamics of glasses composed of organic molecules with photon echo measurements of chromophoric molecules embedded in the glass [21], [22]. Organic glasses used in these studies include ethanol and glycerol, as well as amorphous polymers such as poly methyl methacrylate (PMMA).

These experiments used an HITCI-doped PMMA sample (10 mm diameter, $l = 1$ mm) in a variable-temperature liquid He cryostat. Previous experiments using benchtop lasers had been performed on the ionic xanthine dyes Rhodamine B (RB) and octadecyl Rhodamine B [22]. These experiments provided evidence that electronic dephasing in the intermediate temperature limit ($\sim$4–10 K) was caused by thermal excitation of a $\sim$20 cm^{-1} mode of the polymer matrix. Recently it was shown that ionic dyes can perturb the local structure of a glass [23]. Thus the question arose as to whether this mode was a property of the intrinsic polymer or of the impurity-perturbed polymer surrounding the dye. HITCI, an ionic cyanine dye, has a vastly different structure and size from the xanthine dyes used previously, so any perturbation of its local environment would be very different from that caused by RB [16].

A block diagram of the photon echo apparatus is shown in Fig. 3, reproduced from [16]. The beam from the FEL is converted to its second harmonic at the experimental wavelength of 0.776 μm, at the red edge of the S_0–S_1 absorption band of HITCI, in a 20 mm thick crystal of $LiIO_3$. The conversion efficiency was 25%. The intensity fluctuation of the fundamental beam of $\sim$10% is increased to 20% by frequency doubling. A dichroic beam splitter is used to separate the second harmonic from the fundamental. To improve the stability, the second harmonic is monitored and provides an error signal to an AOM to stabilize the intensity. Fluctuations in the doubled intensity were reduced to $\pm$1% over a time period of hours [16].

A second AOM was used to select single micropulses from the macropulse. Because of the slow micropulse repetition rate (11.8 MHz), this is readily achieved with a rise time of 20 ns. The dependence of the echo decay on pulse repetition frequency was carefully studied. It was found that sample heating limited the number of micropulses during the 2 ms duration macropulse to eight, and the pulse selection frequency during the macropulse was 5 kHz.

A He–Ne laser was made collinear with the FEL output after the second AOM using a dichroic beamsplitter. The He–Ne beam was used to align the subsequent stages of the apparatus. In this way, the maximum amount of experimental alignment could be accomplished in the absence of the FEL beam. Because the FEL output is lo-

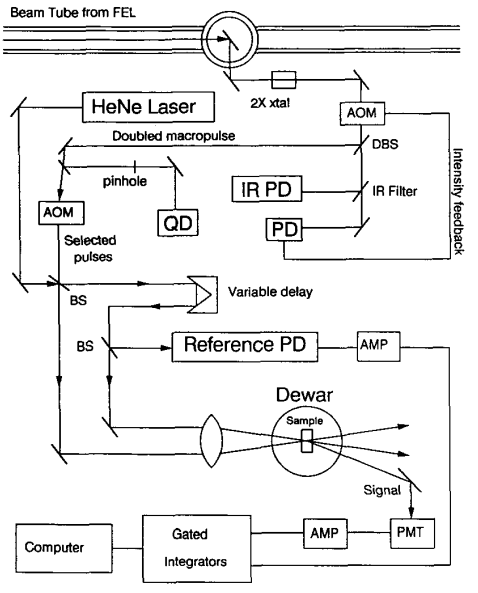

Fig. 3. Block diagram of experimental apparatus for ps photon echo studies using the second harmonic radiation from the SCA/FEL, reproduced from [16]. One acoustooptic modulator (AOM) is used to stabilize the intensity to 1%; a second AOM selects single micropulses from the macropulses. The quad detector QD is used to reproducibly realign the FEL beam. PD = photodiode, BS = beamsplitter, PMT = photomultiplier tube, AMP = operational amplifier.

cated ~80 m from the experimental apparatus, some pointing instabilities of the FEL beam were observed. The fast jitter, roughly ±15% of the beam diameter, was attributed to acoustic vibrations whose effects were amplified by the long optical path. The slower beam drift was attributed to changes in the building temperature. A pinhole and a quad optical detector were used to monitor the position of the FEL beam. Then drift could readily be countered without realigning the entire apparatus by recentering the FEL beam on the quad detector.

The remainder of the setup produces a fixed and a variable delay pulse, which are focused on the sample in an optical cryostat. However, photon echo dephasing in HITCI occurs on the ns time scale, so an optical delay scan of up to 160 cm long, much longer than the autocorrelator in Fig. 1, was required. The two pulses are crossed in the sample at a small angle and focused to a diameter of ~100 μm. Because of wave-vector matching conditions, the photon echo signal pulse propagates in a unique direction so it can be isolated from the two-excitation pulses by a spatial filter. Echo detection is accomplished by a photomultiplier, a gated integrator, and a computer. The optical, cryogenic, and electronic apparatus is shown in Fig. 4.

An experimentally determined photon echo decay curve at 1.5 K is shown in Fig. 5, reproduced from [16]. The fast decay near $\tau = 0$ arises from the broad phonon sideband, whereas the exponential decay with time constant 284 ps reflects the optical dephasing of the zero-phonon line of interest. Temperature-dependent decays obtained

Fig. 4. Photograph of the users' area showing the photon echo apparatus diagrammed in Fig. 3. The FEL beam enters from the left. The optical table is 4′ × 10′. The SHG and AOM assemblies are visible in the foreground. The optical cryostat is at the top right. The 160 cm optical delay line is located at the back of the optical table. Electronic signal analysis equipment and the computer are seen in the background.

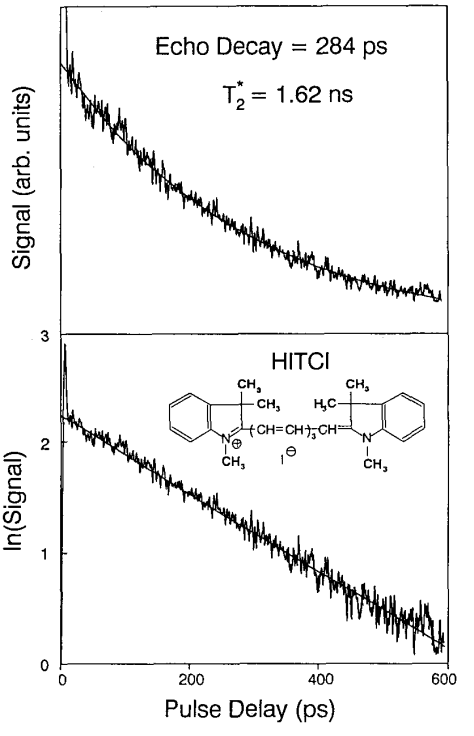

Fig. 5. Picosecond photon echo decay data from the dye HITCI embedded in an amorphous polymeric glass at 1.5 K, reproduced from [16]. The decay is exponential and the decay constant of 284 ps yields a value for the pure dephasing time (lifetime contribution removed) of 1.6 ns.

at 12 temperatures between 1.5 and 10 K showed that in the intermediate temperature regime, optical dephasing was caused by a polymer mode whose frequency was, within experimental error, identical to that observed with RB. Because of significant differences in the structure of HITCI and RB, it could thus be concluded that this mode

is intrinsic to the PMMA polymer itself, rather than arising as a consequence of impurity perturbations [15].

The photon echo experiments were extremely demanding in the requirements they placed on the optical source. An echo experiment depends on the cube of the intensity (in the small flip-angle limit) [19]. Because the experiments were performed with the second harmonic of the FEL wavelength, the actual signal depended on the sixth power of the FEL intensity. Furthermore, as pointed out previously, the stability of the doubled light used in the echo experiments depends not only on the amplitude stability of the FEL but also on the pointing stability, the frequency stability, and the pulse-duration stability. Fluctuations in any of these quantities produce amplitude instability in the doubled light. The data displayed in Fig. 5 is of high quality. In fact, it is as good as photon echo data taken with a conventional lasers operating in the visible part of the spectrum. Over 100 data sets were taken to perform the temperature-dependent study. These were taken over many days and represent many tens of hours of actual data acquisition. During this time the SCA/FEL performed consistently well enough to make the experimental study possible. These experiments demonstrate that is possible to perform complex experiments with an FEL as the source, experiments that are difficult even with conventional lasers.

IV. Pumping and Probing Vibrational Transitions

In this section we discuss quantitatively how an IR FEL can be used to excite and probe molecular vibrational transitions. The goal is to understand under what conditions a large and readily detectable level of vibrational excitation is created. The specific system we have chosen to illustrate these considerations is the molecular material naphthalene $C_{10}H_8$. Naphthalene is chosen for this example because it is among the best characterized molecular solids [24], and a sizable database exists on its properties. The IR transitions in naphthalene may be characterized as moderately intense. They are several orders of magnitude weaker than truly intense transitions such as the electronic states of HITCI, or vibrational transitions of molecules with large dipole moments such as HF.

Naphthalene has 48 normal modes of which 20 are IR active [25]. A vibrational spectrum of naphthalene in the 3–25 μm range is shown in Fig. 6. A vibrational spectrum of this type has enough structure that it provides a *fingerprint* [7] of the molecule. It is possible to identify the constituents of unknown samples via IR spectroscopy by comparison to an atlas of IR spectra [26] and also to confirm the existence of particular functional groups in an unknown molecule. It is often possible to assign particular IR resonances to vibrational excitations of specific structural features of a molecule, e.g., the C–H stretches, C–C stretches, and C–H ($\perp$) bending modes denoted in the figure [25].

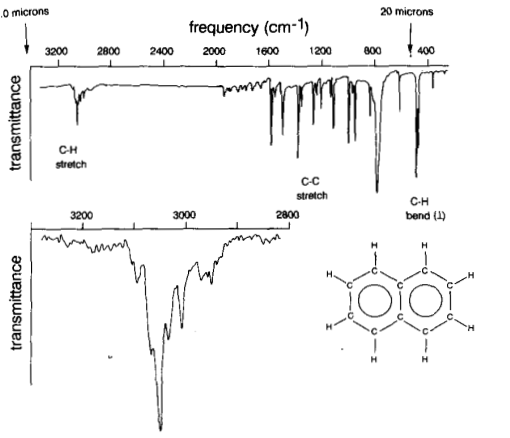

Fig. 6. Infrared transmission spectrum at 298 K of naphthalene microcrystals embedded in a KI pellet. At lower left is a blowup of the C–H stretching region near 3 μm. Experimentally determined values of the absorption cross sections σ_{pk} and transition dipole moments μ are given in Table II.

A. Pumping with an FEL

Tunable IR FEL pulses can be used to produce large levels of excitation in specific mechanical resonances of a given molecule. In many cases of interest, the anharmonicity of the vibrational transition is large enough that a laser tuned to a $0 \rightarrow 1$ transition is not resonant with the $1 \rightarrow 2$ transition. Then the vibrational transition can be treated as a two-state system (TSS). In a bit of simplification, there are two cases of interest. When the dephasing time $T_2 < t_p$, the TSS is driven incoherently toward saturation [18]. When $T_2 > t_p$, the TSS is driven coherently [18]. In either case, it is desirable to produce a sizable population in the excited state, so that n_e/n_g is large, where n_e and n_g denote the number density in the excited and ground states, respectively.

For a pulse duration t_p of a few picoseconds, incoherent pumping will dominate in most condensed phase systems at ambient temperature, in relatively high pressure ($P >$ 10 atm) gas-phase systems, and in low-pressure gases of large [27] molecules. Coherent pumping is possible in a variety of condensed-phase systems at low temperature and for small or intermediate [27] molecules at lower pressures, or in molecular beams.

We now consider how to produce a sizable excitation in two specific states shown in Fig. 6. 1) The most intense C–H stretching mode at 3.28 μm, and 2) a C–C stretching mode at 6.28 μm. The naphthalene spectrum in Fig. 6 provides enough information for a reasonable estimate of n_e/n_g under specific pumping conditions. The naphthalene sample consisted of a suspension of microcrystals in a pellet of KI, a material with good transparency in the IR. This is a useful technique for studying solids, as the concentration of naphthalene can be easily varied to produce the optimal optical density for a particular experiment. Table II summarizes the properties of this sample, which had an optical path length $l = 1$ mm.

TABLE II
NAPHTHALENE PARAMETERS FOR PUMPING CALCULATION[a]

Parameter	3.28 μm (3049 cm^{-1}) $\nu_{41}B_{3u}$ C-H Stretch	6.28 μm (1593 cm^{-1}) $\nu_{31}B_{2u}$ C-C Stretch
Linewidth $\Delta\nu$ @300 K	16 cm^{-1}	6 cm^{-1}
Linewidth[b] $\Delta\nu$ @10 K	—	0.59 cm^{-1}
$-\ln(I/I_0)$ @300 K	0.27	0.81
σ_{pk} @300 K[c]	3.8×10^{-20} cm^2	1.1×10^{-19} cm^2
Dipole moment	0.036 D	0.037 D
Dipole moment	1.19×10^{-31} C-m	1.22×10^{-31} C-m
W_{sat}[d]	1.6 j/cm^2	0.29 J/cm^2
n_e/n_g @300 K[e]	2.4%	12%
θ_v[f]	1170 K	1030 K
Rabi frequency ω_1	3.5×10^{11} rad/s	3.6×10^{11} rad/s
$\theta = \omega_1 t_p$	1.05 rad	1.08 rad
n_e/n_g @10 K[g]	25%	26%

[a]KI pellet, optical path length $l = 0.1$ cm, 2 mg of naphthalene/400 mg of KI, $n = 7.2 \times 10^{19}$ molecules/cm^3.
[b]Taken from [29].
[c]The peak cross section σ_{pk} is given by $-\ln(I_{pk}/I_0) = n\sigma_{pk}l$.
[d]W_{sat}, the saturation fluence, is given by $W_{sat} = h\nu/\sigma_{pk}$.
[e]For incoherent pumping, $n_e/n_g = [1 - \exp(-W/W_{sat})]$.
[f]The vibrational quasi-temperature θ_v is given by $n_e/n_g = [\exp(h\nu/k_B\theta_v) - 1)^{-1}$.
[g]For coherent pumping, $n_e/n_g = \sin^2(\theta/2)$.

TABLE III
FEL MICROPULSE PARAMETERS FOR PUMPING CALCULATION

Parameter	3.28 μm (3049 cm^{-1})	6.28 μm (1593 cm^{-1})
Photon energy	6.1×10^{-20} J/pho	3.17×10^{-20} J/pho
Pulse energy	3 μJ	3 μJ
Beam diameter ($1/e^2$)	100 μm	100 μm
Confocal parameter[a]	4.8 mm	2.5 mm
Fluence, W	380 J/m^2	380 J/m^2
Intensity	1.3×10^{14} W/m^2	1.3×10^{14} w/m^2
Density, ρ	4.3×10^5 J/m^3	4.3×10^5 J/m^3
E field $= (2\rho/\epsilon_0)^{1/2}$	3.1×10^8 V/m	3.1×10^8 V/m

[a]Confocal parameter b is given by $b = 2\pi(\omega_0)^2/\lambda$, where ω_0 is the beam radius.

Table III summarizes the FEL micropulse parameters assumed for this calculation. The 3 μJ energy and 3 ps duration is what one might reasonably expect for the Stanford SCA/FEL with its new injector [17]. It is useful to focus the laser to a small diameter spot, but the confocal parameter should be long relative to the 1 mm sample. Therefore, a reasonable choice is a 100 μm beam diameter. The calculation is simplified by assuming a uniform (rather than Gaussian) beam profile, a rectangular (rather than Gaussian) time envelope, and an optically thin sample.

In the incoherent limit, it is first assumed that $T_1 > t_p > T_2$, where T_1 is the lifetime of the vibrationally excited state. Then the critical parameter is the saturation fluence $W_{sat} = h\nu/\sigma_{pk}$, where σ_{pk} is the peak absorption cross section [19], [28]. The value of σ_{pk} can be determined from Fig. 6, where the abscissa is IR transmittance, from the relation

$$-\ln(I_{pk}/I_0) = n\sigma_{pk}l \tag{3}$$

where I_{pk}/I_0 is the relative intensity of transmitted light at the absorption peak. Table II shows that a typical $\sigma_{pk} \approx 10^{-19}$–$10^{-20}$ cm^2, and a typical $W_{sat} \approx 1$ J/cm^2. The fraction in the excited state is then given by [18], [28]

$$n_e/n_g = [1 - \exp(-W/W_{sat})]. \tag{4}$$

Table II then shows the fractional excitation is of order 2–12% under the assumed conditions. The instantaneous vibrational temperature θ_v [28] is given by

$$n_e/n_g = [\exp(h\nu/k_B\theta_v) - 1]^{-1} \tag{5}$$

so in the cases considered in Table II, $\theta_v \approx 1100$ K.

In the low-temperature limit, it is assumed that $T_1 \geq T_2 > t_p$. That is certainly the case for the C–C stretching mode in Table III, where $T_2 = 9$ ps [29]. The critical parameter for coherent excitation is the Rabi frequency $\omega_1 = \mu E/\hbar$, where μ is the transition dipole moment and E is the laser pulse electric field [19]. The value of μ for a given transition can be estimated from its spectral width $\Delta\nu$ in Fig. 6 because [19], [30]

$$\mu^2 \propto \int d\lambda\, \sigma(\lambda) \approx \pi\Delta\nu\sigma_{pk}. \tag{6}$$

The values of μ determined from Fig. 6 for both transitions in Table II of $\mu \approx 0.04$ D are by coincidence approximately equal. Together with the electric field [31] of $E \approx 3 \times 10^8$ V/m in Table III, the value of $\omega_1 \approx 3 \times 10^{11}$ rad/s is determined. Then a 3 ps pulse produces a flip angle of $\theta \approx 1$ rad, and for the C–C stretch an excitation fraction $n_e/n_g \approx 25\%$ is predicted. This favorable result suggests that a variety of coherence experiments such as photon echoes should be possible with an FEL performing as in Table III. The principal reason that a greater excited state fraction is produced at low temperature is the narrowing of the IR transition on cooling the sample. This narrowing effect produces a larger value of σ_{pk}, which causes the molecular transition to interact more strongly with the IR pulse.

B. Probing with an FEL

The state being probed after vibrational excitation may be the *same* state excited by the pump pulse, so that pump and probe are the same color, or it may be a *different* state, in which case a second color [28] is required for the probe pulse. Saturation recovery and photon echoes are one color experiment that probes either the vibrational energy relaxation (VR) characterized by T_1 (saturation recovery), or the homogeneous dephasing lifetime characterized by T_2 (photon echoes). Two-color experiments can be used to monitor the appearance of the excess vibrational energy in a different state than the one being pumped [28], [32]–[33].

In order to perform two-color experiments, the two pulses must be *synchronized*. That is easily achieved when one pulse is the FEL fundamental and the other is produced by SHG. This technique is useful when the precise frequency of the second pulse is not important. However,

some experiments require two independently tunable pulses. Schwettman and Smith have discussed a novel scheme that would permit an SCA/FEL to produce optical pulses with two independently tunable frequencies [11]. Another possibility that seems easier to implement is the synchronization of a conventional ps pulse laser to the FEL. This possibility limits the wavelength of the second pulse to regions accessible to such lasers, i.e., the visible or near UV. Synchronization of two independent lasers requires that the spacing between micropulses is identical within an integral factor and that phase noise be eliminated. The former requirement may be easily met with an actively mode-locked laser [6] as the FEL and conventional laser can be driven by the same frequency source. Merely using the same frequency source does not guarantee synchronization. However, experience with dual-mode locked lasers suggests that this synchronization can be readily achieved with the use of active phase-locking circuitry [6], [34], [35].

In the saturation recovery experiment, the pump pulse produces a transient bleaching of the sample, which is observed as a temporary decrease in the absorbance of the weaker probe pulse by the sample. The observed change in absorbance with delay (τ) is given by

$$\Delta A(\tau) = A_0[1 - \exp(-W/W_{sat})] \exp(-\tau/T_1) \quad (7)$$

where A_0 is the unsaturated absorbance at the probe wavelength. In (7) it is assumed that 1) A_0 is small so that W is constant through the length l of the sample, 2) the pulses have uniform spatial profiles that overlap perfectly throughout the sample, 3) the anharmonicity of the vibrational transition is large enough to treat it as a TSS, and 4) the TSS interacts weakly with the bath of other vibrational states, and relaxation of the excited level returns the TSS directly to its ground state. The first three factors affect only the magnitude of ΔA, whereas strong coupling to the bath may lead to a nonexponential time dependence. With a properly stabilized FEL, and some signal averaging, the observation of ΔA values of a few percent should present no major problems.

Hartmann *et al.* [19] have discussed in detail the procedure for calculating the intensity of a photon echo signal. We need only note that the photon echo is a coherently emitted pulse in a unique direction whose intensity can, in some circumstances, be as great as a few percent of the pump pulse intensity. In practice, photon echo detection is rarely limited by the echo intensity but rather by the background caused by a small portion of the pump pulses, which are scattered by the sample into the detector, and which therefore cannot be removed by spatial or spectral filtering. IR photon echoes are likely to suffer less from scattered light compared to visible photon echoes because the intensity of this background drops off as λ^{-4} for some forms of scattered light.

One promising application of the two-color technique is to use the second color as a Raman probe of excitations in states other than the state being pumped [28], [32]. Raman scattering from vibrationally excited states produces incoherent anti-Stokes emission at a frequency $\nu_L + \nu_v$, where ν_L is the frequency of the incident laser line and ν_v the frequency of the excited vibration [18]. Anti-Stokes Raman is not produced by ground vibrational states. The number $N_{aS}(\theta)$ of anti-Stokes Raman photons per second scattered into a detector is given by [28]

$$N_{aS}(\theta) = In_eV\theta(d\sigma_R/d\theta) \quad (8)$$

where $(d\sigma_R/d\theta)$ is the differential Raman cross section, I is the incident laser intensity, n_e the number density of excited vibrations in the irradiated volume V, and θ the solid angle subtended by the detector. A typical $f/4$ monochromator has $\theta = 0.05$ sr, and a large differential cross section is of order $d\sigma_R/d\theta = 10^{-29}$ cm^2 · sr [19], [28]. Table II shows that the Raman cross section is $< 10^{-10}$ of the IR cross section, so that this technique relies on obtaining a large average power from the FEL. Detailed numerical results are presented in [28], and discussed briefly below.

V. Selected Applications

In a previous article, we discussed some potential applications of a proposed two-color FEL system. In light of the experience gained from the photon echo experiments, we have had several conversations with FEL developers and potential FEL users, and we have identified several new and potentially important applications not discussed previously. The applications discussed below share one feature in common: based on our experience and detailed numerical calculations, all of these applications should be feasible using a one-color system that performs as well as the SCA/FEL at Stanford. This list of applications is not meant to be exhaustive. It is somewhat biased in the direction of condensed matter dynamics by our personal interests, although we also consider gas-phase experiments. Finally, it may be possible to perform some of the suggested experiments with a laboratory benchtop system, but in general we have tried to consider problems that cannot easily be studied without the advantages offered by an FEL, and we have indicated why we believe this to be the case.

A. Vibrational Dynamics

Practically all chemical processes in condensed phases and in the gas phase involve vibrational excitations and vibrational energy transfer within a molecule or among adjacent molecules. There are four broad categories of interest: 1) vibrational relaxation (VR), 2) vibrational cooling (VC), 3) vibrational dephasing, and 4) the relationship between vibrational relaxation and chemical reaction dynamics. VR refers to *loss* of excess energy from an initially prepared excited state, characterized by T_1. Energy is lost to the surrounding bath in condensed phases and by collisions in the gas phase. Large molecules have many different vibrational levels, thus excitation of a high frequency vibration usually results in a series of VR steps, or vibrational cascade, before all the initial excess energy

is dissipated. This multistep process is called VC [29], [36]. Understanding VC requires a knowledge of the rate of energy loss from the initial state and the rate parameters for all intermediate states. Thus two-color experiments are particularly useful for VC studies. Vibrational dephasing refers to the loss of phase coherence of the excited state [32]. In isolated molecules, dephasing occurs via the interaction of the initial state and a bath consisting of other, isoenergetic states [27]. In condensed phases, dephasing occurs via T_1 processes, or via pure dephasing [32], [37] caused by stochastic interactions with the bath. Coherence loss may be investigated by a variety of optical coherence measurements including free-induction decay or photon echo [20].

Given the paucity of knowledge about vibrational dynamics in condensed matter, there is a wide range of problems open to study. Some systems of current interest include collective vibrational excitations of single crystals, mechanical excitations of amorphous systems such as organic glasses and polymers, and excitations localized on molecular impurities in crystalline or amorphous materials. Surface states present a great challenge because the concentration of surface states is small at full (i.e., monolayer) coverage, and coverage dependence extending to submonolayers is also of interest. It is desirable to extend the kind of studies that have been performed on well-characterized crystalline materials [37]–[39] to systems of biochemical or biomedical significance, e.g., hemoglobin, photosynthetic units, or viruses, and to study the interaction of tunable IR pulses with hard and soft tissues.

A number of groups are at this time actively investigating VR of solids [39] and surfaces [40], [41] using IR saturation recovery with 1–5 μm benchtop lasers. Vibrations in this region involve motions of the light atoms H or D, and a few other groups or molecules, notably CO. VR studies with the FEL are therefore important in the lower frequency region where heavier atoms are involved. Larger molecules have an abundance of lower frequency modes that involve skeletal motions or conformational changes of functional importance. The intermediate frequency modes (6–25 μm) are generally the longest-lived modes in molecular solids [37]. These are the bottleneck states that trap energy during VC [36]. The lowest frequency modes (20–100 μm) are the doorway vibrations through which energy enters and leaves the molecule. They involve large amplitude displacements and can often be implicated in chemical reactivity [42]. The low-frequency modes associated with the bond between a surface and an adsorbed molecule may also lie in this frequency range.

Two-color experiments that will detect vibrations populated by energy transfer from the initial state are much more difficult than saturation recovery experiments. Nevertheless, these proposed experiments would provide a unique picture of vibrational energy flow through the molecule, a problem currently of great importance in condensed matter chemistry. Two-color experiments demand a high average power source, so even with vibrational excitation in the 1–5 μm range, benchtop laser systems are inadequate. The most immediate method of obtaining two colors is by SHG, so the simplest arrangement for a VC experiment involves IR pumping and incoherent anti-Stokes probing. Then the fact that the SHG probe wavelength cannot be tuned independently from the IR pump is of little consequence. Raman probing, although hindered by the small Raman cross section is advantageous because several Raman active modes can be studied simultaneously.

A block diagram of this type of experiment is shown in Fig. 7. The sample is held at low temperature so the thermal anti-Stokes background scattering is negligible. A key element of this apparatus is an optical multichannel analyzer, consisting of a cooled CCD detector and spectrograph. These detectors have near unit quantum efficiency in the 0.4 to 1 μm range, and a dark noise equivalent to a few photons per hour. Because the Raman signal is so weak, it is important that one or two-photon fluorescence from the sample be minimized. A probe in the 0.8 to 1.0 μm range is ideal. In this apparatus, the pump pulse wavelength is constrained to be $\nu_L \leq 4$ μm, because after two stages of SHG, the probe pulses must lie in a region accessible to the detector. Conversion efficiency into the fourth harmonic is dependent on the SHG material, but a reasonable estimate is 2–20%. The probe may be generated instead by a synchronized laser, ideally a mode-locked Ti:sapphire laser, to lift all constraints from the pump.

Numerical estimates of the signal strength are encouraging using numbers appropriate for the naphthalene sample used to generate the spectrum in Fig. 6, where $n_g = 7 \times 10^{19}/\text{cm}^3$. Then for $n_e/n_g = 3\%$ (e.g., Table II), $n_e = 2 \times 10^{18}/\text{cm}^3$, and $V = 8 \times 10^{-6}$ cm^3. At 825 nm, 1 mW of probing light focused on the excited volume produces an intensity $I = 5.3 \times 10^{19}$ photons/cm^2/s, so a strong Raman cross section of $(d\sigma_R/d\theta) = 10^{-29}$ cm$^2 \cdot$ sr and an $f/4$ spectrograph will give roughly 50 photons/s of anti-Stokes Raman emission per milliwatt of probing light.

This result is quite conservative because the intensity of probing light is likely to be more than 10 mW, and the excitation probability at low temperature is likely to exceed 3%. The probability of excitation transfer from the initial IR-active state to the lower energy Raman-active state was assumed above to be unity. At first glance this estimate may seem overoptimistic, but the VC process has a peculiar property: during some portions of the VC process, vibrational occupation numbers increase with time. For example, in the theoretical model of Hill and Dlott [36], unit excitation of a C–H stretch at 3057 cm^{-1} produced an occupation number of practically unity in the strongly Raman active 511 cm^{-1} mode at $\tau = 200$ ps because the 3057 cm^{-1} excitation created several vibrational excitations that then became trapped in the long-lived 511 cm^{-1} state.

Successful two-color experiments of this type on model systems might eventually lead to a new development of

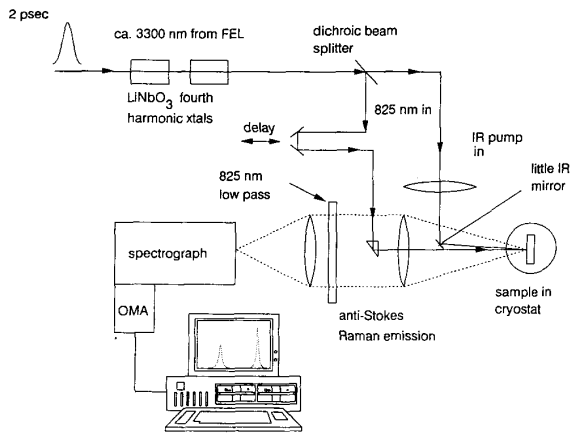

Fig. 7. Block diagram of proposed experimental apparatus that can be used for two-color IR pump, anti-Stokes Raman probing experiments on molecular solids. The same apparatus can be used for hyper-Raman spectroscopy. OMA denotes an optical multichannel analyzer consisting of a cooled CCD detector.

potentially great importance, namely two-dimensional IR (2D-IR) spectroscopy. Two-dimensional spectroscopy is used to simplify the absorption spectrum of a complicated molecule or aggregate and to investigate interactions among different functional groups. The specific 2D scheme in mind is similar in concept to 2D magnetic resonance. It follows from the ability of powerful IR pulses from the FEL to create a large enough vibrational excitation that its influence can be detected in other vibrations of the same molecule or a neighboring molecule.

For a specific example, consider again the naphthalene spectrum in Fig. 6, and the two-color configuration discussed above. Notice in Fig. 6 that the C–H stretching region of naphthalene consists of several unresolved peaks. The pump laser is scanned through the C–H stretching region while a specific anti-Stokes Raman emission is detected from one lower frequency vibration. One might expect that the different C–H stretching vibrations will interact more or less strongly with the probed state. Only those C–H stretching modes that transfer energy efficiently to the probed state will be observed in this simplified spectrum, therefore the resulting 2D spectrum of the C–H stretching region will appear less complex than the ordinary IR spectrum. If signal-to-noise considerations permit, the extension of this method to other more complicated systems such as proteins could be a powerful new way of understanding molecular mechanics.

Infrared optical coherence experiments probe in detail the dynamical interactions responsible for the finite linewidth of IR transitions. For example, IR spectroscopy has proven to be a useful tool to study molecules adsorbed on surfaces, but it was not until the photon echo measurements of Guyot-Sionnest *et al.* [41], on Si–H adsorbed on the surface of silicon, that the extent of inhomogeneous broadening of a surface state could be determined quantitatively. A related problem concerns the relation between surface coverage and vibrational dynamics. Detailed investigation at low-surface coverage seems to require a high average power IR laser like the FEL.

In the photon echo experiments previously described, the dynamical behavior of amorphous organic solids was investigated via the optical dephasing of a chromophore embedded in the glass. The FEL results helped clarify the issue of how the chromophore perturbed the local structure of the polymer. Infrared pulses from the FEL will eventually obviate the use of chromophoric impurities as photon echoes can be performed directly on the vibrational IR transitions of the glass itself, resulting in a knowledge of the intrinsic dynamics of the chemically unperturbed glass.

B. Hyper Raman Scattering

Infrared absorption and Raman scattering are the two principal tools of vibrational spectroscopy. Hyper-Raman scattering (HRS) is an emerging tool in chemical applications [43], [44], which is complementary to both IR and Raman. Ordinary Stokes Raman scattering appears at the frequency $\nu_L - \nu_v$, whereas HRS appears at $2\nu_L - \nu_v$. The HRS cross section is extremely small but increases with laser power I, so in analogy to (8),

$$N_{\mathrm{HR}}(\theta) = In_g V\theta[I(d\sigma_{\mathrm{HR}}/d\theta)] \tag{9}$$

where $N_{\mathrm{HR}}(\theta)$ is the number of hyper-Raman photons per second at the detector, and the term in the brackets is the power-dependent cross section. A typical HRS cross section is $(d\sigma_{\mathrm{HR}}/d\theta) \approx 10^{-64}$ cm^4 · s · sr/photon [43]. To obtain a probability of HRS that is comparable to ordinary Raman scattering would require a laser intensity of 10^{35} photons/cm^2/s, corresponding to roughly 10^{16} W/cm^2. But, with ps pulses, 10^{12} W/cm^2 is the practical limit to avoid sample damage, so HRS requires not only high peak power but also a high average power source. An FEL operating in the 1–2 μm range seems an ideal candidate for HRS studies. Then the hyper-Raman emission at 0.5–1 μm will be compatible with CCD detectors. The experimental apparatus for HRS is simply a spectrograph with a CCD and an FEL.

For many high-symmetry molecules, HRS permits the observation of vibrational transitions that are forbidden by symmetry in either Raman or IR [43]. Naphthalene, which belongs to symmetry group D_2^h, has 48 normal modes of which 24 are Raman active, 20 are IR active, and the remaining 4, of a_u symmetry, are inactive. These inactive transitions are not forbidden by symmetry in HRS.

Recently it has been shown that molecules adsorbed on the surface of roughed metal surfaces [43] or colloidal particles [44] can exhibit surface-enhanced HRS (SEHRS), in analogy to the well-known surface-enhanced Raman scattering (SERS) [43]. The enhancement factor for SEHRS is approximately 10^{13}, compared to the roughly 10^6 factor for SERS [43]. The additional enhancement factor makes it possible to observe the weaker HRS effect even from low-concentration surface adsor-

bates. SEHRS is apparently more sensitive to the orientation of the adsorbed molecule on the surface than either IR or SERS [43], [44]. However, the mechanism of this additional enhancement factor is currently unknown. Controversies about the mechanism of SERS have been put to rest by observing the dependence of the enhancement factor on the laser frequency ν_L for different metal particles [45]. To repeat these studies in HRS would require an extremely powerful, tunable near-IR laser. The FEL is, therefore, the most important existing tool that can be brought to bear on this problem.

C. Nanoheating

Nanoheating refers to experiments where a laser is used to produce a brief but enormous jump in temperature localized at a specific nanometer scale object, typically in a mixture or assembly of other objects. By using an IR pulse tuned into resonance with the chosen object, nearby objects are heated solely by thermal conduction. When an ultrashort pulse is used, the heating rate might exceed the rate of thermal conduction, producing an enormous temperature jump at the chosen object with weak, indirect effects on the surroundings. However, little is currently known about heat transfer over nanometer length scales [46], particularly in molecular materials [47], so further work needs to be done to understand nanoheating processes in detail.

The attraction of using an ultrashort pulse FEL in nanoheating studies is frequency agility. Because of the desire to obtain selective heating, and the trade-off between heating and thermal conductivity, a good deal of effort must go into determining the optimal wavelength for nanoheating processes.

Nanoheating in a moderate pressure gas is straightforward. For perhaps 15 years it has been recognized that an IR laser can drive isolated molecules into dissociation [48]. The best studied example of this IR multiphoton dissociation process is the use of a CO_2 laser to dissociate SF_6 gas. Although researchers were initially disappointed to find this process was not bond specific, i.e., it could not (except in certain remarkable examples [49]) produce a product other than that obtained by simple heating, it is clear that IR dissociation can be *species specific*. So in a low-pressure mixture of SF_6 and other gases, the SF_6 can be made to dissociate with an IR laser tuned into the intense SF_6 absorption while the other molecules remain cold. In this perhaps trivial example, heating is confined to 1-nm sized feature on a collisional time scale, typically 100 ps at STP.

Recently, there have been a number of emerging commercial applications for this process [50]. Due to the great cost of tunable IR photons, these applications are limited to processes where a few photons produce a large quantity of reaction products. An obvious example is isotope separation. In uranium, the ratio of U^{238} to U^{235} is about 150:1, so a few IR photons can purify 150 U atoms. A less obvious example is the initiation of radical chain reactions, where a laser-produced radical can initiate the chain reaction of many thousands of molecules. Laser production of radical initiators in gas-phase reaction vessels can be far more productive than thermal production of radicals because the overall heating of the reaction mixture is reduced, leading to fewer undesirable side reactions [50].

Another example is selective surface desorption [51]. Molecules on a surface can be desorbed by raising the temperature. In temperature-programmed desorption, a mass spectrograph is used to study the composition of the gas desorbed from a surface while the temperature is steadily increased. Ordinarily the molecules with the weakest adsorption bonds leave the surface first. The desorbed molecules may then consist of weakly bound species or the decomposition products of more strongly bound species.

It may be possible to desorb one component of a mixture with an IR laser tuned in resonance with a vibrational transition of that component. Because these resonant IR photons are absorbed preferentially by a single species, initially the absorbed energy is localized over nm-sized regions on the surface, provided the molecules are present at submonolayer coverage. However, if vibrational relaxation and thermal conduction are rapid compared to desorption, the laser would merely heat the surface uniformly thus ultrashort pulses are more likely to produce selective desorption [51].

We close this section with two potentially important but speculative applications of nanoheating: viral vaccine production and cell fusion. One method for producing viral vaccines is thermal inactivation. Viruses consist of a protein coat that is recognized by the immune system and that stimulates the production of antibodies and an inner core of nucleic acid that provides a template for viral replication. A virus with its nucleic acid core inactivated, but its protein coat intact, can stimulate antibody production in a host, but it cannot replicate—it is a vaccine. Certain viruses, such as those that cause AIDS, have labile protein coats that are thermally converted into unrecognizable forms before the nucleic acid core can be inactivated. Thermal inactivation is ineffective with this type of virus.

Fig. 8, reproduced with permission from Thomas *et al.* [52], shows a laser Raman spectrum of a virus, denoted MS2. In this paper, the virus spectrum was compared to the spectra of the individual coat and RNA components to assign the spectral transitions as indicated. The point of this spectrum is that well-resolved Raman transitions corresponding to either the coat proteins or the RNA core can be readily observed in the 6–16 μm range. Because water has a relative window of transparency in this range, it is reasonable to assume that corresponding IR transitions in this region can be found—thus it is possible to imagine irradiating viral suspensions with FEL pulses tuned to RNA transitions. It is then possible that nanoheating with picosecond IR pulses can localize thermal denaturation effects at the nucleic acid core without a

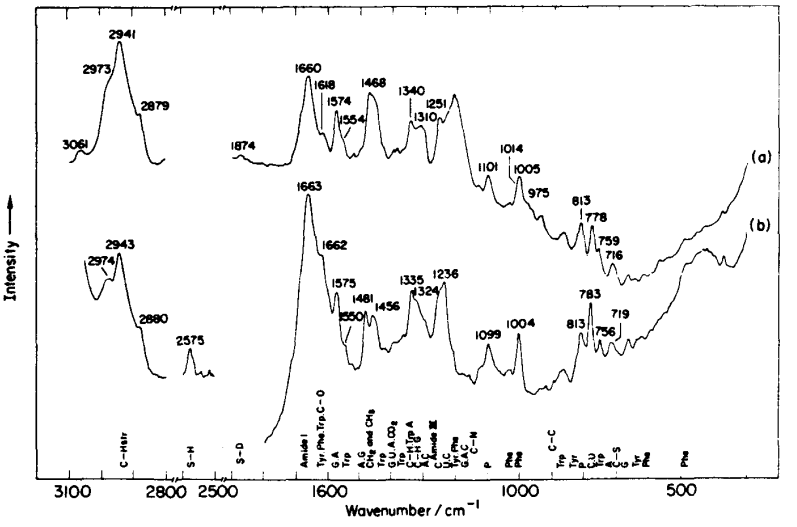

Fig. 8. Laser Raman spectrum of an aqueous suspension of the MS2 virus in (a) H_2O and (b) D_2O, reproduced with permission from [52]. In the 6–15 μm region, several well-resolved transitions can be observed and assigned to either the protein coat or the RNA core. For example, the intense peak at 1660 (1663) cm^{-1} is due to the Amide III stretch of the protein backbone, whereas the sharp band at 778 (783) cm^{-1} is a vibrational mode of the cytosine–uracil base pair of the RNA.

large-scale effect at the protein coat, which is cooled by the surrounding aqueous medium.

Cell fusion is a novel method of transferring genetic material or other cell constituents between two cells. A recent advance in nondestructive cell manipulation involves the use of laser tweezers [53]. A cell in aqueous suspension can be trapped by radiation pressure in a focused laser beam. Using a few milliwatts of power from a continuous Nd:YAG laser focused to a waist of a few microns, cells can be readily moved and pairs of cells brought in contact with no apparent adverse effects, as seen in Fig. 9.

Merely bringing a pair of cell membranes in contact will not permit the exchange of most materials. A schematic diagram of a pair of contacted membranes is also shown in Fig. 9. The matchsticks represent amphiphilic molecules in the membrane [54]. The head is a hydrophilic group that preferentially orients toward the aqueous suspension inside the cell and the aqueous medium outside the cell. The tail is a hydrocarbon and therefore in the hydrophobic group. Water-soluble components such as proteins and nucleic acids will not pass readily through the hydrophobic phase. Therefore transfer of components requires merging the cells, i.e., cell fusion. Successful cell fusion requires a means of creating an aperture through the common membrane interface. FEL nanoheating might provide such a tool.

To achieve cell fusion, it is important to limit radiation effects to the vicinity of the membrane, as otherwise genetic damage to the cells can occur. The hydrophobic components such as cholesterol and the hydrocarbon groups on the phosphatides, which account for up to 50% of typical mammalian cell membranes [54], have distinct IR transitions [55] that might permit a tunable IR pulse to produce a large temperature jump localized at the membrane.

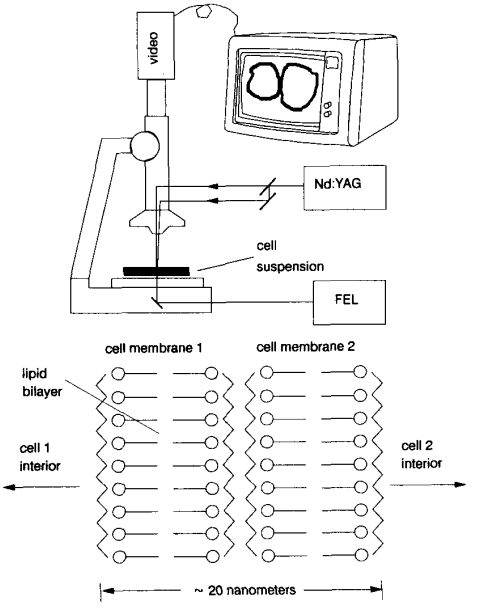

Fig. 9. Proposed apparatus for cell fusion experiments by nanoheating of the cell membrane. Top: Two cells in aqueous suspension are brought in contact using Nd:YAG laser tweezers and observed under a microscope. An FEL tuned to infrared resonances of the cell membrane is used to specifically heat the membrane. Bottom: a schematic diagram of two cell membranes in contact. The matchsticks denote amphiphilic molecules. The heads are polar and hyrophilic; the tails are nonpolar and hydrophobic. The hydrophobic constituents of the membrane show IR absorption lines distinct from other, water-soluble components of the cell.

The remarkable features of nanoheating are the brief duration of the temperature jump and the possibility of creating enormous transient temperatures. For an optically thin structure such as a membrane or virus, the instantaneous temperature jump ΔT caused by a short pulse of fluence W is given by

$$\Delta T = W\alpha/C \tag{10}$$

where α is the absorption coefficient ($\alpha = n_g \sigma_{pk}$) and C is the heat capacity. The temperature jump ΔT may easily be *hundreds or thousands of degrees*. Specifically, typical heat capacities range from 2 J/g/deg (hydrocarbons) to 4 J/g/deg (water). A typical hydrocarbon density $n_g \approx 10^{22}$ cm^{-3}, so for a cross section $\sigma_{pk} = 10^{-19}$ cm^2 as in naphthalene (Table II), $\alpha \approx 10^3$ cm^{-1}. A 3 μm, 1 μJ pulse focused through a typical microscope objective with numerical aperture (NA) = 0.65 will produced a focused spot diameter of order $\lambda/\text{NA} = 5$ μm, so the maximum achievable value of $W = 5$ J/cm^2. Equation (10) then shows that ΔT may be as large as 2500° for the hydrocarbon component of a membrane.

For the membrane geometry diagrammed in Fig. 9, the characteristic length l for cooling due to thermal transfer to the surrounding aqueous medium is about 20 nm. A large, thin hot sheet immersed in a colder liquid will obey a cooling law of the approximate form

$$\Delta T(t) = \Delta T(0) \exp\left[(-2\kappa/l^2 C)t\right] \tag{11}$$

where κ is the thermal conductivity. For water, $\kappa = 6$ mW/cm/deg, so the characteristic time for cooling, $\tau_c = Cl^2/2\kappa = 1.5$ ns. It should be kept in mind this τ_c is an upper limit because thermal diffusion was assumed dominate. Over nm-length scales, some of the excess mechanical energy is transported by ballistic phonons [46], [47], which propagate at velocities of ~3 nm/ps and would therefore leave the membrane region in 10 ps.

For successful cell fusion to occur, the membrane bilayer structure must be disrupted by the heat pulse without killing the cells. Ordinarily, this type of bilayer undergoes a transition to a disordered or melted state well below 100°C, but little is known about the time dependence of melting. In order to melt the membrane on the ns time scale, a somewhat greater temperature may be required. It should, however, be possible to melt the membrane without large-scale denaturation of the transmembrane proteins because of the short duration of the heat pulse. Although protein denaturation and membrane melting occur at similar temperatures, it should take longer to denature proteins, which have a hydrogen-bonded secondary structure, than to melt the membrane. If IR pulse heating can be initially confined to the membrane, then the remainder of the cell is heated only indirectly by conduction. If the membrane is taken to be a physical shell 20 nm thick, then for a 2 μm diameter cell, the ratio $V_{\text{cell}}/V_{\text{membrane}} \approx 20$. Because only one-half of the heat flow from the membrane is in the direction of the cell interior, a membrane temperature jump of $\Delta T = 200$ degrees will increase the temperature of the cell by only 5°.

A nanoheating experiment requires a short, coherent IR pulse but little energy or average power. An FEL is preferable over a benchtop laser system for initial experiments because it is critical to survey a wide range of wavelengths in order to maximize the heating of the chosen feature while minimizing heating of the surrounding material. The consequences of nanoheating events are difficult to predict. It is a potentially exciting new area for experimental investigation.

VI. Concluding Remarks

The current state of FEL development indicates that the first important applications to basic research will involve IR ps pulse FEL's. We have confined our discussions to a few selected example applications involving solids, surfaces, gas dynamics, and biological systems, but clearly the ideas we have discussed have wide applicability. An FEL can be used in extremely simple applications as a cutting or welding tool. We have considered applications requiring FEL's that are true spectroscopic tools, i.e., they produce pulses with well-defined temporal and spectral characteristics. It is now clear that some FEL designs, e.g., the SCA/FEL at Stanford University, can fulfill these requirements. The principal obstacle in developing FEL's for this type of work seems to lie in producing a stable, near-transform limited pulse that remains locked onto a narrow molecular transition for an extended period of time without a substantial reduction in the average or peak intensity of the FEL.

Experience acquired using an FEL for ps photon echo spectroscopy demonstrates that sophisticated application projects can indeed be performed at an FEL users' facility but only if certain conditions are met. Sharing an FEL appears to be much more difficult than sharing a synchrotron light source, thus a given FEL may not be able to service a large number of users at the same time. Because an FEL is not by itself an experiment, users must have considerable resources, including equipment and space, to perform their experiments. The user's experiment may be on the order of the complexity of the FEL itself. There is a virtually unlimited potential for FEL applications in the area of condensed matter dynamics and biomedical processes. However, prudence dictates that FEL applications of this type are only reasonable if they cannot be performed by a readily available benchtop laser system. We have discussed a number of such applications that require either the high average power of the FEL, the remarkable ability of the FEL to survey a wide range of wavelengths, or the ability to produce intense pulses to the red of 5 μm, where good benchtop systems are not yet available.

The interactions between FEL users and FEL developers at Stanford resulted in remarkable and synergistic effects. The demands of the users for well-characterized and transform-limited pulses with high-amplitude stability led to an improved understanding of frequency instabilities of the FEL, the development of an external cavity amplitude stabilization scheme that could produce $\pm 1\%$

amplitude stability in the doubled light, and unique data concerning the dynamics of amorphous organic solids.

Extremely close interactions between users and FEL operators is absolutely necessary if applications of the type discussed here are to be realized. Most users will initially have little experience with the unique aspects of the FEL beam, whereas the FEL operator will usually have little experience in the expectations of the user. The best way to meet these expectations is have on hand a wide variety of time and frequency-domain diagnostics to ensure the FEL performance is well characterized and understood by the user and the FEL operators and that the characteristics are matched to the experimental task at hand [17].

Acknowledgment

We gratefully acknowledge many useful conversations with Prof. H. A. Schwettman and Prof. T. I. Smith of Stanford University, S. Greenfield of Stanford University, Prof. A. J. Sievers of Cornell University, Prof. B. Tromberg of Beckman Laser Institute and Medical Clinic, University of California, Irvine, and Prof. R. P. Van Duyne of Northwestern University. I.-Yin Sandy Lee obtained the IR spectrum of naphthalene.

References

[1] "Proceedings of the 11th international free-electron laser conference," *Nucl. Instrum. Methods Phys. Res A*, vol. 296, 1990.

[2] See, e.g., *J. Opt. Soc. Amer. B*, vol. 6, no. 5, 1989, Special Issue on Physics of Free-Electron Laser Applications.

[3] "Free-electron lasers and application," in *Proc. Soc. Photo-Opt. Instrum. Eng.*, vol. 1227, 1990.

[4] K-J. Kim and A. Sessler, "Free-electron lasers: Present status and future prospects," *Science*, vol. 250, no. 1, pp. 88–93, 1990.

[5] C. B. Harris, *Ultrafast Phenomena VII*, Springer Ser. Chem. Phys., vol. 53. E. P. Ippen, G. A. Mourou, and A. H. Zewail, Eds., New York: Springer-Verlag, 1990.

[6] G. R. Fleming, *Chemical Applications of Ultrafast Spectroscopy*. Oxford: Oxford Univ. Press, 1986.

[7] F. A. Cotton, *Chemical Applications of Group Theory, Second Edition*. New York: Wiley-Interscience, 1971.

[8] E. B. Wilson, Jr., J. C. Decius, and P. C. Cross, *Molecular Vibrations, The Theory of Infrared and Raman Vibrational Spectra*. New York: Dover, 1955.

[9] A. P. Pierce, M. A. Dahleh, and H. Rabitz, "Optical control of quantum-mechanical systems: Existence, numerical approximation, and applications," *Phys. Rev. A.*, vol. 37, no. 12, pp. 4950–4964, 1988.

[10] W. J. Tomlinson, R. H. Stolen, and C. V. Shank, "Compression of optical pulses chirped by self-phase modulation in fibers," *J. Opt. Soc. Amer. B.*, vol. 1, no. 2, pp. 139–149, 1984.

[11] H. A. Schwettman and T. I. Smith, "Two-color free-electron laser driven by a radio-frequency linear accelerator," *J. Opt. Soc. Amer. B.*, vol. 6, no. 5, pp. 973–976, 1989.

[12] M. D. Perry, O. L. Landen, J. Weston, and R. Ettlebrick, "Design and performance of a high-power, synchronized Nd:Yag-dye laser system," *Opt. Lett.*, vol. 14, no. 5, pp. 42–44, 1989.

[13] A. Laubereau, L. Greiter, and W. Kaiser, "Intense tunable picosecond pulses in the infrared," *Appl. Phys. Lett.*, vol. 25, no. 1, pp. 8789, 1974, also S. R. Shen, Ed., *Non-linear Infrared Generation*. Berlin: Springer-Verlag, 1977.

[14] See the discussion and references in D. J. Bradley, "Methods of generation," in *Ultrashort Light Pulses. Picosecond Techniques and Applications, 2nd ed.*, S. L. Shapiro, Ed., Topics in Applied Physics, vol. 18. New York: Springer-Verlag, 1984, pp. 18–82.

[15] S. R. Greenfield, Y. S. Bai, and M. D. Fayer, "Optical dephasing of a near infrared dye in PMMA: Photon echoes using the superconducting accelerator pumped free electron laser," *Chem. Phys. Lett.*, vol. 170, no. 2,3, pp. 133–138, 1990.

[16] Y. S. Bai, S. R. Greenfield, M. D. Fayer, T. I. Smith, J. C. Frisch, R. L. Swent, and H. A. Schwettman, "Picosecond photon echo experiments using a superconducting accelerator pumped free electron laser," *J. Opt. Soc. Amer. B*, vol. 8, no. 8, pp. 1652–1656, 1991.

[17] T. I. Smith, J. C. Frisch, R. Rohatgi, H. A. Schwettman, and R. L. Swent, "SCA/FEL status," in *Proc.*, 11th Int. Free-Electron laser conf., *Nucl. Instrum. Methods Phys. Res A*, vol. 296, no. 1, 1990.

[18] A. Yariv, *Quantum Electronics; 2nd ed.* New York: Wiley, 1975.

[19] I. D. Abella, N. A. Kurnit, and S. R. Hartmann, "Photon echoes," *Phys. Rev.*, vol. 141, no. 2, pp. 391–406, 1966.

[20] M. D. Levenson and S. S. Kano, *Introduction to Nonlinear Laser Spectroscopy*. New York: Academic, 1988; J. I. Steinfield, *Molecules and Radiation*. Cambridge: MIT Press, 1986.

[21] C. A. Walsh, M. Berg, L. R. Narasimhan, and M. D. Fayer, "Probing intermolecular interactions with picosecond photon echo experiments," *Acct. Chem. Res.*, vol. 20, pp. 120–140, 1987; L. R. Narasimhan, K. A. Littau, D. W. Pack, Y. S. Bai, A. Elschner, and M. D. Fayer, "Probing organic glasses at low temperature with variable time scale optical dephasing measurements," *Chem. Rev.*, vol. 90, no. 3, pp. 439–457, 1990.

[22] ——"A picosecond photon echo study of a chromophore in an organic glass: Temperature dependence and comparison to nonphotochemical hole burning," *J. Chem. Phys.*, vol. 86, pp. 77–87, 1987; A. Elschner, L. R. Narasimhan, and M. D. Fayer, "High temperature optical dephasing mechanism for dye molecules in PMMA glass," *Chem. Phys. Lett.*, vol. 171, no. 1, pp. 19–24, 1990.

[23] D. W. Pack, L. R. Narasimhan, and M. D. Fayer, "Solvation shell effects and spectral diffusion: Photon echo and optical hole burning experiments on ionic dyes in ethanol glass," *J. Chem. Phys.*, vol. 92, no. 7, pp. 4125–4138, 1990.

[24] A. I. Kitaigorodskii, *Molecular Crystals and Molecules*. New York: Academic, 1973.

[25] E. R. Lippincott and E. J. O'Reilly, "Vibrational spectra and assignment of naphthalene and naphthalene-d-8," *J. Chem. Phys.*, vol. 23, no. 2, pp. 238–244, 1955.

[26] H. A. Szymanski, *Interpreted Infrared Spectra*. New York: Plenum, 1964.

[27] J. D. McDonald, "Creation and disposal of vibrational energy in polyatomic molecules," *Annu. Rev. Phys. Chem.*, vol. 30, no. 1, 29–50, 1979.

[28] D. D. Dlott and M. D. Fayer, "Application of a two-color free-electron laser to condensed-matter molecular dynamics," *J. Opt. Soc. Amer. B*, vol. 6, no. 5, pp. 977–994, 1989.

[29] J. R. Hill, E. L. Chronister, T.-C. Chang, H. Kim, J. C. Postlewaite, and D. D. Dlott, "Vibrational relaxation and vibrational cooling in low temperature molecular crystals," *J. Chem. Phys.*, vol. 88, no. 2, pp. 949–967, 1988.

[30] A. P. Thorne, *Spectrophysics*. London: Chapman and Hall, 1974.

[31] W. H. Flygare, *Molecular Structure and Dynamics*. Englewood Cliffs, NJ: Prentice-Hall, 1978

[32] A. Laubereau and W. Kaiser, "Vibrational dynamics of liquids and solids investigated by picosecond light pulses," *Rev. Mod. Phys.*, vol. 50, pp. 607–665, 1978.

[33] T.-C. Chang and D. D. Dlott, "Picosecond vibrational cooling in mixed molecular crystals studied with a new coherent Raman scattering technique," *Chem. Phys. Lett.*, vol. 147, no. 1, pp. 18–24, 1988.

[34] D. Cotter, "Technique for highly stable active mode-locking," D. H. Auston and K. B. Eisenthal, Eds., in *Ultrafast Phenomena IV*, Springer Ser. Chem. Phys., vol. 38. New York: Springer-Verlag, 1984, pp. 78–80.

[35] J. F. Kauffmann, M. J. Cote, P. G. Smith, and J. D. McDonald, "Novel circuit for phase locking two mode-locked lasers," *Rev. Sci. Instrum.*, vol. 60. no. 1, pp. 281–283, 1989; V. J. Newell, F. W. Deeg, S. R. Greenfield, and M. D. Fayer, "Tunable subpicosecond dye laser amplified at 1 kHz by a cavity-dumped Q-switched, and mode-locked Nd:YAG laser," *J. Opt. Soc. Amer. B*, vol. 6, no. 2, pp. 257–263, 1989.

[36] J. R. Hill and D. D. Dlott, "A model for ultrafast vibrational cooling in molecular crystals," *J. Chem. Phys.*, vol. 89, no. 2, pp. 830–841, 1988; J. R. Hill and D. D. Dlott, "Theory of vibrational cooling in molecular crystals: Application to crystalline naphthalene," *J. Chem. Phys.*, vol. 89, no. 8, pp. 842–858, 1988; D. D. Dlott, "Ultrafast vibrational energy transfer in the real world: Laser ablation, energetic solids, and hemeproteins," *J. Opt. Soc. Amer. B*, vol. 7, no. 4, pp. 1638–1652, 1990.

[37] D. D. Dlott, "Dynamics of molecular crystal vibrations," in *Laser Spectroscopy of Solids II*, W. Yen, Ed., Topics in Applied Physics, vol. 65. Berlin: Springer-Verlag, 1989, pp. 167–200.

[38] —— "Dynamics of molecular crystal vibrations," *Annu. Rev. Phys. Chem.*, vol. 37, no. 1, pp. 157–187, 1986.
[39] W. E. Moerner, A. J. Sievers, and R. Chraplyvy, "Anharmonic relaxation times of molecular vibrational modes in alkali halide crystals," *Phys. Rev. Lett.*, vol. 47, no. 7, pp. 1082–1085, 1981; M. Harig and H. Dubost, "Infrared transient antihole burning in the 1 → 2 vibrational transition of $^{12}C^{17}O$ in solid N_2: Evidence for energy-dependent spectral transfer," *Phys. Rev. Lett.*, vol. 49, no. 5, pp. 715–718, 1982; D. M. Kammen, T. R. Gosnell, R. W. Tkach, and A. J. Sievers, "Vibrational relaxation dynamics of matris-isolated $BH_2D_2^-$," *J. Chem. Phys.*, vol. 87, no. 4, pp. 4371–4375, 1987.
[40] E. J. Heilweil, M. P. Casassa, R. R. Cavanagh, and J. C. Stevenson, "Picosecond vibrational energy relaxation of surface hydroxl groups on colloidal silica," *J. Chem. Phys.*, vol. 81, no. 3, pp. 2856–2858, 1984; E. J. Heilweil, M. P. Casassa, R. R. Cavanagh, and J. C. Stevenson, "Vibrational deactivation of surface OH chemisorbed on SiO_2: Solvent effects," *J. Chem. Phys.*, vol. 82, no. 6, pp. 5216–5231, 1985; J. D. Beckerle, M. P. Casassa, R. R. Cavanagh, and E. J. Heilweil, "Ultrafast infrared response of adsorbates on metal surfaces: Vibrational lifetimes of CO/Pt(111)," *Phys. Rev. Lett.*, vol. 64, no. 6, pp. 2090–2093, 1990; A. L. Harris, L. Rothberg, L. H. Dubois, N. J. Levinos, and L. Dhar, "Molecular vibrational energy relaxation at a metal surface: Methyl thiolate on Ag(111)," *Phys. Rev. Lett.*, vol. 64, pp. 2086–2089, 1990.
[41] P. Guyot-Sionnest, P. Dumas, Y. J. Chabal, and G. S. Higashi, "Lifetime of an adsorbate substrate vibration: H on Si(111)," in *Ultrafast Phenomena VII*, C. B. Harris, E. P. Ippen, G. A. Mourou, and A. H. Zewail, Eds., Springer Ser. Chem. Phys. vol. 53. pp. 374–376; P. Guyot-Sionnest, "Coherent processes at surfaces: Free-induction decay and photon echo of the Si-H stretching vibration for H/Si(111)," *Phys. Rev. Lett.*, vol. 66, no. 11, pp. 1489–1492.
[42] D. D. Dlott and M. D. Fayer, "Shocked molecular solids: Vibrational up pumping, defect hot spot formation and the onset of chemistry," *J. Chem. Phys.*, vol. 92, no. 6, pp. 3798–3812, 1990.
[43] J. T. Golab, J. R. Sprague, K. T. Carron, G. C. Schatz, and R. P. Van Duyne, "A surfaced enhanced hyper-Raman scattering study of pyridine adsorbed onto silver: Experiment and theory," *J. Chem. Phys.*, vol. 88, pp. 7942–7951, 1988.
[44] C. K. Johnson and S. A. Soper, "Nonlinear surface-enhanced spectroscopy of silver colloids and pyridine: Hyper-Raman and second-harmonic scattering," *J. Phys. Chem.*, vol. 93, no. 21, pp. 7281–7285, 1989.
[45] R. P. Van Duyne, "Laser excitation of Raman scattering from adsorbed molecules on electrode surfaces," in *Chemical and Biochemical Applications of Lasers Vol. 4*, C. B. Moore, Ed. New York: Academic, 1978, pp. 101–186; H. Metiu, "Surface enhanced scattering," *Prog. Surface Sci.*, vol. 17, pp. 153–320, 1984.
[46] P. Klemens, "Thermal conductivity and lattice vibrational modes," *Solid St. Phys.*, vol. 7, no. 1, pp. 1–96, 1958; D. D. Joseph and L. Preziosi, "Heat waves," *Rev. Mod. Phys.*, vol. 61, no. 1, pp. 41–72, 1989.
[47] H. Kim and D. D. Dlott, "Molecular dynamics simulation of nanoscale thermal conduction and vibrational cooling in a crystalline naphthalene cluster," *J. Chem. Phys.*, vol. 94, no. 12, pp. 8203–8209, 1991.
[48] P. A. Schulz, Aa. S. Sudbo, D. J. Krajinovich, H. S. Kwok, Y. R. Shen, and Y. T. Lee, "Multiphoton dissociation of polyatomic molecules," *Annu. Rev. Phys. Chem.*, vol. 30, no. 1, pp. 379–410, 1979; C. D. Cantrell, Ed., *Multiple-Photon Excitation and Dissociation of Polyatomic Molecules*. Berlin: Springer-Verlag, 1986.
[49] R. L. Vander Wal, J. L. Scott, and F. F. Crim, "Selectively breaking the oxygen-hydrogen bond in water-d," *J. Chem. Phys.*, vol. 92, no. 2, pp. 803–805, 1990.
[50] R. L. Woodin, D. S. Bomse, and G. W. Rice, "Lasers in chemical processing," *Chemical and Engineering News*, vol. 69, no. 51, pp. 20–31, Dec. 17, 1990.
[51] N. J. Tro, D. A. Arthur, and S. M. George, "Infrared free-electron laser as a probe of vibrational dynamics on surfaces," *J. Opt. Soc. Amer. B*, vol. 6, no. 5, pp. 995–1002, 1989.
[52] G. J. Thomas, Jr., B. Prescott, P. E. McDonald-Ordzie, and K. A. Hartman, "Studies of virus structure by laser-Raman spectroscopy. II. MS2 phage, MS2 capsids and MS2 RNA in aqueous solutions," *J. Mol. Biol.*, vol. 102, no. 1, pp. 103–124, 1976.
[53] W. H. Wright, G. J. Sonek, Y. Tadir, and M. W. Berns, "Laser trapping in cell biology," *IEEE J. Quantum Electron.*, vol. 26, pp 2148–2157, 1990.
[54] F. Wold, *Macromolecules: Structure and function*. Englewood Cliffs, NJ: Prentice-Hall, 1976.
[55] R. J. H. Clarke and R. E. Hester, Eds., *Spectroscopy of Biological Systems, Advances in Spectroscopy*, vol. 13. New York: Wiley, 1986.

Dana D. Dlott was born in Los Angeles, CA, on September 11, 1952. He received the B.A. degree in chemistry from Columbia University, NY, in 1974, and the Ph.D. degree also in chemistry from Stanford University, Stanford, CA, in 1979.

In 1979, he joined the faculty of the School of Chemical Sciences at the University of Illinois, Urbana. He is currently an Associate Professor of chemistry. His research is concerned with ultrafast dynamics of complex, condensed phase systems, vibrational relaxation, shock-wave induced chemical reactions, electron transfer, biophysics and chemical reactions of proteins, laser ablation and optical damage, and laser-induced processes in imaging science.

Dr. Dlott is a member of Alpha Chi Sigma, the American Chemical Society, the Optical Society of America, and the American Association for Advancement of Science. From 1983 to 1985, he was an Alfred P. Sloan Fellow.

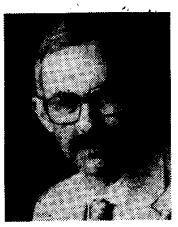

Michael D. Fayer was born in Los Angeles, CA, on September 12, 1947. He received the B.S. and Ph.D. degrees in chemistry from the University of California, Berkeley, in 1969 and 1974, respectively.

In 1974, he joined the Department of Chemistry at Stanford University where he is currently a Professor of chemistry. His research is concerned with dynamics and intermolecular interactions in complex molecular systems. His research group is involved in the investigation of liquids, liquid crystals, glasses, crystals, polymeric solids, thin films, flames, heat and acoustic propagation, photoinduced electron transfer, and electronic excitation transport.

Dr. Fayer was an Alfred P. Sloan Fellow, a Dreyfus Foundation Fellow, a Guggenhein Fellow, and he is a Fellow of the American Physical Society. He serves on the Editorial Board of the *Journal of Chemical Physics*, is an Associate Editor of the *Journal of Luminescence*, and an Advisory Editor for *Chemical Physics and Chemical Physics Letters*. He is a member of Sigma Xi, the American Chemical Society, the American Physical Society, and the American Association for Advancement of Science.